A Trajectory-based Bumpless Switching Control of Multi-Evaporator Air-Conditioning Systems

Tushar Jain

Abstract

Multiple-evaporator/vapor compression cooling systems are used for air conditioning in multi-zone buildings with a refrigerant supplied to each individual zone-evaporator from a central compressor/condenser unit. Such systems, incorporating controlled electronic expansion valves associated to each evaporator and a variable-speed compressor, allow the overall system to be able to operate in different modes in order to achieve cooling requirements and energy efficiency. Switching between the different modes associated with the cooling demands might give rise to switching transients. Such transients are likely to negatively impact the control performance and consequently the energy efficiency of the overall system. In this paper, a novel technique is proposed for dealing with such transients when switching between control modes in a multiple-evaporator/vapor compression cooling system in order to ensure that the control performance undergoes no degradation. The proposed approach is purely a "data-driven" technique using only the plant input/output measurements available in real-time. A simulated experiment with a two-evaporator/vapor compression cooling system shows that the proposed algorithm can achieve a quite satisfactory overall performance under mode switching.

I. Introduction

An emerging building space air conditioning technology is the variable refrigerant flow (VRF) technology based on the classical vapor compression cycle [1], [3], [6]. The vapor compression cooling cycle is a simple four stage thermodynamics process that cools a room or an enclosed space to a temperature lower than the surroundings.

Strong requirements on energy saving and the growing end-user demand for air conditioning system that has independent units serving different zones in a building makes multi-evaporator variable refrigerant flow system the ideal candidate for many applications such as commercial buildings, offices and hotels. A multi-evaporator VRF system, also called multi-split VRF system, is a cooling system consisting of one outdoor unit, i.e. the condenser, and multiple indoor units, i.e. the evaporators. Such systems are best suited for variable thermal load applications since their design is based on inverter technology, i.e. a variable frequency drive, which adapts the speed of the compressor to the varying thermal loads in the building. Moreover, a pulse modulating valve called an electronic expansion valve (EEV), in each unit controls the exact amount of refrigerant to be injected into each indoor unit in order to maintain the zone air temperature at the set-point. In addition, such systems are instrumented with temperature sensors and pressure sensor which permanently monitor the amount of superheat across indoor unit evaporators, hereby ensuring a safe operation of the system. The VRF system can efficiently distribute cooling capacity to keep up with changing loads with respect to the time of the day, room occupancy, solar loads, etc. [1] The VRF system might, therefore, operates in different modes, such as, for example, the modes in which all the indoor units are operating or modes in which selected indoor units are turned off. For an efficient operation of the overall system, the control laws should be adapted to the different cooling modes. A typical approach to such control law adaptation at run time is the off-line design of a bank of controllers where each controller of the bank is associated to a mode of the system. When all these controllers are packed into a control processor, controller switching is used to adapt the controller to changing operating points. Clearly, some way of switching between the controller as the system evolves is required. This issue of transferring control authority between different controllers is not a trivial task, and due to its practical importance, it has received a lot of attention from the research community over several years, see e.g. [7], [11] and references therein. Upon switching, the control signal is imposed by a new controller and some kind of coherence must be enforced between the output trajectory of the new controller and that of the former controller in order to ensure that no undesirable transient takes place which in the case of the VRF air-conditioning system may negatively impact the control performance (as evidenced e.g. by the comfort of the users in the rooms) and also the energy efficiency of the overall system. The avoidance of these transients upon switching is commonly known as the bumpless transfer problem. The benefits of using a VRF air conditioning system as evidenced by its adaptation to various capacity indoor units with added value with regards to comfort levels and reduced power consumption can be severely jeopardized if control mode switching are not taken care of. Unfortunately, there has been little work on managing mode-switching transients in such air-conditioning systems, except the work recently reported in [8], [9]. In this work concerning a dual-evaporator air conditioning system, the authors present the design and application of a model-based compensator for dealing with mode switching similar to the model-based anti-windup compensator derived in [7]. A shortcoming of this approach is clearly the fact that the switching transients management relies on a known model of the system at switching time which might not be available as it is usually the case in practical applications.

In this paper, we propose a new bumpless switching algorithm for the control of a VRF system for a two-zone building which gets rid off of the above mentioned modeling issue. The novelty of this algorithm lies in the fact that we do not use any

[1]Tushar Jain is with Aalto University, School of Chemical Technology, P. O. Box 16100, 00076 AALTO, Finland tushar.jain@aalto.fi

a priori knowledge of the model of the plant in real-time. We use the mathematical framework of behavioral theory to design the bumpless switching mechanism. The paper is organized as follows. Section 2 gives the basics of the behavioral approach needed throughout. The data-driven bumpless switching approach is developed in section 3. Finally, section 4 presents the two-zone VRF benchmark system and its control modes with the simulation of the data-driven bumpless switching mechanism to illustrate the features of the algorithm.

II. Preliminaries on feedback in the behavioral framework

In the behavioral setting, feedback is viewed as the interconnection of two dynamical systems, namely the plant and the controller. A Linear Time-Invariant (LTI) dynamical system Σ is described by a triple $\Sigma = (\mathbb{T}, \mathbb{S}, \mathcal{B})$ where $\mathbb{T} \subseteq \mathbb{R}$ is the time axis, $\mathbb{S} \subseteq \mathbb{R}^{\mathtt{s}}$ is the signal space, with $\mathbb{R}^{\mathtt{s}}$ denoting the $\mathtt{s}$-dimensional real Euclidean vector space over the field of real numbers $\mathbb{R}$, and $\mathcal{B} \subseteq \mathbb{S}^{\mathbb{T}}$ is the *behavior*. The set $\mathbb{S}$ is the space in which the system variables take on their values and the behavior $\mathcal{B}$ is a family of $\mathbb{S}$-valued time trajectories, where a trajectory is a function $s : \mathbb{T} \to \mathbb{S}, t \mapsto s(t)$ and $\mathtt{s}$ denotes the number of components in s. Let $S(\xi) \in \mathbb{R}^{\bullet \times \mathtt{s}}[\xi]$, and consider the following system of constant coefficient differential equations

$$S\left(\frac{d}{dt}\right) s = 0. \tag{1}$$

where $\mathbb{R}^{\bullet \times \mathtt{s}}[\xi]$ is the set of polynomial matrices with indeterminate ξ having an unspecified number of rows (of course, finite) and $\mathtt{s}$ number of columns. Then the behavior $\mathcal{B}$ is the set of solutions of the finite system (1) which is defined as

$$\mathcal{B} = \{s \in (\mathbb{R}^{\mathtt{s}})^{\mathbb{T}} | \text{ equation (1) satisfies}\}.$$

Representation (1) is called a kernel representation of $\mathcal{B}$ and sometimes, we denote the behavior as $\mathcal{B} = \mathtt{ker}(S(\frac{d}{dt}))$.

The interconnection of two dynamical systems is often dealt in the so-called full interconnection in which all system variables take part in the interconnection. Consider two dynamical systems $\Sigma_1 = (\mathbb{T}, \mathbb{S}, \mathcal{B}_1)$ and $\Sigma_2 = (\mathbb{T}, \mathbb{S}, \mathcal{B}_2)$ with the common time axis $\mathbb{T}$, and the common signal space $\mathbb{S}$. The interconnection of Σ_1 and Σ_2 is defined by $\Sigma_1 \wedge \Sigma_2 = (\mathbb{T}, \mathbb{S}, \mathcal{B}_1 \cap \mathcal{B}_2)$, where $\mathcal{B}_1 \cap \mathcal{B}_2 = \{s | s \in \mathcal{B}_1 \text{ and } s \in \mathcal{B}_2\}$. Here, $\wedge$ denotes the interconnection of two systems, while $\cap$ denotes the intersection of the behaviors of the two systems. In terms of kernel representations, let Σ_1 be described by $R_1(\xi)s = 0$, and Σ_2 by $R_2(\xi)s = 0$. Then, $\Sigma_1 \wedge \Sigma_2$ is described by $\begin{bmatrix} R_1(\xi) \\ R_2(\xi) \end{bmatrix} s = 0$. In this way, a dynamical system imposes restrictions on another dynamical system such that the interconnected system satisfies the laws of both systems.

Consider $\mathcal{P}$ denotes the behavior of the plant, and $\mathcal{C}$ denotes the behavior of the controller with system variable $s = (r^T, y^T, u^T)^T$. In the sequel, we sometimes denote this column vector by $s = \mathtt{col}(r, y, u)$. Given their kernel representation, these behaviors are defined as

$$\mathcal{P} = \{s \in (\mathbb{R}^{\mathtt{s}})^{\mathbb{T}} | R(\xi)s = 0\}, \mathcal{C} = \{s \in (\mathbb{R}^{\mathtt{s}})^{\mathbb{T}} | C(\xi)s = 0\} \tag{2}$$

The interconnection of $\mathcal{P}$ and $\mathcal{C}$ yields the controlled behavior $\mathcal{K}$, which is defined as $\mathcal{K} = \left\{s \in (\mathbb{R}^{\mathtt{s}})^{\mathbb{T}} | s \in \mathcal{P} \text{ and } s \in \mathcal{C}\right\}$. In this case, we say that for the given $\mathcal{P}$, $\mathcal{K}$ is implemented by $\mathcal{C}$ or "$\mathcal{C}$ implements $\mathcal{K}$". The following result from [13, Lemma 3.5] gives the implementability condition on $\mathcal{K}$.

Theorem 1: The behavior $\mathcal{K}$ is implementable w.r.t. $\mathcal{P}$ by the full interconnection if and only if $\mathcal{K} \subset \mathcal{P}$

Control problems are always specified by certain criterion, which single out specific sub-behaviors as desirable. Here, such specification is defined in terms of the system variable, and we call it the desired behavior $\mathcal{D} \in (\mathbb{R}^{\mathtt{s}})^{\mathbb{T}}$. In terms of a kernel representation, it is defined by $\mathcal{D} = \mathtt{ker}(D(\xi))$, where $D(\xi)$ is a polynomial matrix. Therefore, the control problem turns into synthesizing a controller $\mathcal{C}$ for the given $\mathcal{P}$ and $\mathcal{D}$ such that when it interconnects with the plant, the interconnected system satisfies the desired behavior.

In our data-driven bumpless switching approach to be presented in the next section, we do not have any access to, or use of, *a priori* plant parameters, i.e. the matrix $R(\xi)$ is *not available* during the design of the bumpless mechanism. Precisely, our interest lies in synthesizing this bumpless mechanism without using the polynomials matrix $R(\xi)$. It is a fact that the given desired behavior should be implementable otherwise no controller can achieve the desired specifications. So from theorem 1, we should have the following implementability condition on $\mathcal{D}$ as $\mathcal{D} \subset \mathcal{P}$..

III. Data-driven bumpless switching algorithm

A switched-mode control structure employing a set of N controllers $\mathbb{C} = \{\mathcal{C}_1, \mathcal{C}_2, ..., \mathcal{C}_N\}$ is constructed where it is assumed that in each plant mode, one of the controller makes the desired behavior $\mathcal{D}$ implementable when the pairing of the plant and that controller is considered as a stand-alone feedback system. At run-time, a supervisor determines which controller must be selected in the set $\mathbb{C}$ in order to achieve the desired behavior. Though the pairing of each controller with a corresponding plant mode might be viewed as stand-alone feedback, the overall evolving system is actually an hybrid system. Throughout it is assumed the controllers (possibly, in their kernel form) and the supervisor are given at the outset and our aim is to devise a real-time mechanism which ensures that the overall hybrid system satisfies to the desired behavior at any time.

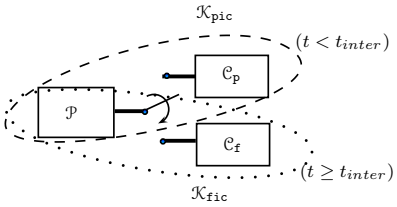

Fig. 1. Switching a controller

From now on, we will make reference to a time-dependent subset of the behavior $\mathcal{P}$. This time-dependent subset, denoted as $\mathcal{P}_m^t$, is characterized by the set of signals experimentally measured on the time interval $(-\infty, t]$ where t is the current time. More precisely, let (u_m, y_m) be the input/output (of the real plant) actually measured in an experimental setting, as e.g. in an actual closed-loop setting, then this subset $\mathcal{P}_m^t$ of the behavior $\mathcal{P}$ is defined by

$$\mathcal{P}_m^t = \left\{ s = (r, u, y) \in \mathbb{S}^T \ s.t. \ \begin{pmatrix} u(\tau) - u_m(\tau) \\ y(\tau) - y_m(\tau) \end{pmatrix} = 0 \ \text{ for all } \tau \in (-\infty, t] \right\} \tag{3}$$

With this definition, it is clear that $\mathcal{P}_m^t \subseteq \mathcal{P}$ for all $t \in (-\infty, \infty)$.

Consider the scenario illustrated in figure 1, where $\mathcal{C}_{\mathtt{p}}$ is the past controller with which the measurement set $\mathcal{P}_m^t$ is formed and a controller $\mathcal{C}_{\mathtt{f}}$, i.e. the future controller, is switched in the loop. It is well known that whenever an instantaneous switching of a controller is performed in real-time at $t = t_{\mathtt{inter}}$, undesirable transients might appear in the closed-loop that significantly deteriorates the control performance [4]. It is argued in [14] that the main cause behind the appearance of these undesirable transients, called bumps, is the lack of dynamical consistency between the "state trajectory" of the controller $\mathcal{C}_{\mathtt{f}}$ before and after the switching or interconnection instant $t = t_{\mathtt{inter}}$. Our objective is therefore to switch $\mathcal{C}_{\mathtt{f}}$ in the running closed-loop system in a way such that the overall controlled behavior still satisfies the *desired* behavior. When controller switching is achieved in this way, we qualify it as a bumpless switching. To make precise this notion, let $\mathcal{K}_{\mathtt{pic}}$ and $\mathcal{K}_{\mathtt{fic}}$ denote the past interconnected system and the future interconnected system respectively and $t_{\mathtt{inter}}$ is the time at which controller switching takes place,

$$\mathcal{K}_{\mathtt{pic}} = \{(r, y, u) | (r, u, y) \in \mathcal{P} \text{ and } (r, y, u) \in \mathcal{C}_{\mathtt{p}}\} \forall t < t_{\mathtt{inter}}$$
$$\mathcal{K}_{\mathtt{fic}} = \{(r, y, u) | (r, u, y) \in \mathcal{P} \text{ and } (r, y, u) \in \mathcal{C}_{\mathtt{f}}\} \forall t \geq t_{\mathtt{inter}}.$$

Definition 1: The switching of controller $\mathcal{C}_{\mathtt{f}}$ in the feedback loop with the running plant $\mathcal{P}$ is said to be bumpless whenever $\mathcal{K}_{\mathtt{fic}} \subseteq \mathcal{D}$.

Clearly, controller switching is bumpy if it leads to closed-loop signals which no longer belong to the desired behavior. The next proposition, which is a main result of this paper, is of paramount importance and will be the basis for the derivation of the algorithm in achieving bumpless switching.

Proposition 1: Let $\mathcal{D}$ be an implementable desired behavior and consider the controller switching scenario as depicted in figure 1. Then, the switching of controller $\mathcal{C}_{\mathtt{f}}$ in the closed-loop with the running plant $\mathcal{P}$ is bumpless if there exists a trajectory $\tilde{r}$ such that $\tilde{s} = (\tilde{r}, u_m, y_m) \in \mathcal{P}_m^t \cap \mathcal{C}_{\mathtt{f}} \subseteq \mathcal{D}$ for all $t < t_{\mathtt{inter}}$.

Proof: Let s_{f} be the trajectory of the closed-loop switched-mode system after t_{inter}, i.e., after switching $\mathcal{C}_{\mathtt{f}}$ in the loop. Then, under the stated condition, the achievability of a real-time smooth interconnection of $\mathcal{C}_{\mathtt{f}}$ with $\mathcal{P}$ at time t_{inter} is trivially equivalent to the fact that the following concatenated signal, denoted s, and defined by

$$s = \tilde{s} \diamond_{t_{\mathtt{inter}}} s_{\mathtt{f}} \Longleftrightarrow s(t) = \begin{cases} \tilde{s}(t) & t < t_{\text{inter}} \\ s_{\mathtt{f}}(t) & t \geq t_{\text{inter}} \end{cases} \tag{4}$$

should belongs to the desired behavior, i.e.,

$$\mathcal{D} \ni s = \tilde{s} \diamond_{t_{\text{inter}}} s_{\mathrm{f}} \tag{5}$$

Clearly, the membership relationship (5) implies $s_{\mathrm{f}} \in \mathcal{D}$, which means that the controller switching is actually bumpless. ■

Remark 1: First, it is worth noticing that proposition 1 implicitly introduces a "*virtual*" behavior, i.e., a set of signals $\tilde{s} = (\tilde{r}, u_m, y_m)$ corresponding to a loop in which $\mathcal{C}_{\mathtt{f}}$ and $\mathcal{P}$ are fictively connected before time t_{inter} (though in reality $\mathcal{P}$ is connected with $\mathcal{C}_{\mathtt{p}}$ for all $t < t_{\text{inter}}$). Second, the significance of proposition 1 is that in order to achieve bumpless switching when $\mathcal{C}_{\mathtt{f}}$ will be effectively switched in the loop for all $t \geq t_{\text{inter}}$, this *virtual* loop should already satisfies the desired behavior $\mathcal{D}$.

In the proof of proposition 1, the membership relationship (5) is exhibited as the main requirement for achieving a real-time smooth interconnection. Therefore, the question arises as: under what condition, the relationship (5) holds?

To answer this question, we need more information on the behavior of the system. Observe that, thanks to remark 1, the trajectory (4) might be viewed as that of the closed-loop system consisting of $\mathcal{C}_{\mathtt{f}}$ being constantly in the loop since ever and forever. This trajectory is in fact splitted at $t = t_{\text{inter}}$ in two parts, that is, a past trajectory and a future trajectory. Although

these manifest trajectories may be the main signals of immediate interest, there may be additional independent variables in the system which allow a more complete description of the behavior. In particular, for a future trajectory in the behavior $\mathcal{D}$ to be a continuation of a past trajectory in $\mathcal{D}$ obviously would require some boundary conditions to be met at the splitting time. These boundary conditions can be expressed through the aforementioned independent variables which are usually called the state of the system. The manifest trajectories might therefore be explicitly parametrized with these new independent variables (i.e., the state) so as to catch all the information about the past which are relevant to do a continuation of the trajectory in the future. It can be proved that such a parametrization always exists [10]. Let us denote the state of the virtual closed-loop and future behavior of the system respectively by $\tilde{\ell}$ and ℓ_{f} and parametrize explicitly the manifest trajectory of the virtual closed-loop and future manifest trajectory with respect to their states as $\tilde{s}(\tilde{\ell})$ and $s_{\mathrm{f}}(\ell_{\mathrm{f}})$. The following lemma which is a direct consequence of the property of the state answers the raised question above.

Lemma 1: Let the manifest trajectories $\tilde{s}(\tilde{\ell})$ and $s_{\mathtt{f}}(\ell_{\mathtt{f}})$ be elements of the behavior $\mathcal{D}$, then their concatenation at time $t = t_{\mathtt{inter}}$ also belongs to $\mathcal{D}$ if $\tilde{\ell}(t^-_{\mathtt{inter}}) = \ell_{\mathtt{f}}(t^+_{\mathtt{inter}})$.

As we are dealing with behaviors of controlled systems consisting in the interconnection of a plant $\mathcal{P}$ and a controller $\mathcal{C}$, the state ℓ of the controlled behavior $\mathcal{P} \cap \mathcal{C}$ is a vector which can be partitioned explicitly as $\ell = \begin{bmatrix}(\zeta^{\mathcal{P}})^T & (\zeta^{\mathcal{C}})^T\end{bmatrix}^T$ where $\zeta^{\mathcal{P}}, \zeta^{\mathcal{C}}$ are respectively the states of the plant and the controller. Thanks to this partitioning, the state of the virtual closed-loop behavior $\mathcal{P}^t_m \cap \mathcal{C}_{\mathtt{f}}$ for $t \in (-\infty, t_{\mathtt{inter}})$ is written as $\tilde{\ell} = \begin{bmatrix}(\tilde{\zeta}^{\mathcal{P}})^T & (\tilde{\zeta})^T\end{bmatrix}^T$ and the state of the future behavior as $\ell_{\mathtt{f}} = \begin{bmatrix}(\zeta^{\mathcal{P}}_{\mathtt{f}})^T & (\zeta_{\mathtt{f}})^T\end{bmatrix}^T$ for all $t > t_{\mathtt{inter}}$. Introduce the (past) state $\ell_{\mathtt{p}} = \begin{bmatrix}(\zeta^{\mathcal{P}}_{\mathtt{p}})^T & (\zeta^{\mathcal{C}_{\mathtt{p}}})^T\end{bmatrix}^T$ of the actual loop $\mathcal{P}^t_m \cap \mathcal{C}_{\mathtt{p}}$ evolving on the time axis $(-\infty, t_{\mathtt{inter}})$, then clearly $\tilde{\zeta}^{\mathcal{P}} = \zeta^{\mathcal{P}}_{\mathtt{p}}$. It is a well-known fact [2] that despite a possible discontinuity of the manifest variables (attached to $\mathcal{P}$) at the switching instant $t_{\mathtt{inter}}$, the state of the plant is continuous at $t = t_{\mathtt{inter}}$, i.e., $\zeta^{\mathcal{P}}_{\mathtt{p}}(t^-_{\mathtt{inter}}) = \zeta^{\mathcal{P}}_{\mathtt{f}}(t^+_{\mathtt{inter}})$ which implies that $\tilde{\zeta}^{\mathcal{P}}(t^-_{\mathtt{inter}}) = \zeta^{\mathcal{P}}_{\mathtt{f}}(t^+_{\mathtt{inter}})$. From the above, it turns out that the boundary condition $\tilde{\ell}(t^-_{\mathtt{inter}}) = \ell_{\mathtt{f}}(t^+_{\mathtt{inter}})$ in lemma 1 is achieved if and only if $\tilde{\zeta}(t^-_{\mathtt{inter}}) = \zeta_{\mathtt{f}}(t^+_{\mathtt{inter}})$. This means that the state of the to-be-switched controller $\mathcal{C}_{\mathtt{f}}$ should be initialized at the switching instant $t = t_{\mathtt{inter}}$ with the value $\tilde{\zeta}(t^-_{\mathtt{inter}})$ of the state that controller $\mathcal{C}_{\mathtt{f}}$ would have achieved, had it been in the loop on the (past) time interval $(-\infty, t_{\mathtt{inter}})$.

Next, the question arises of how to compute explicitly the state ζ of a controller when the controller is given by its kernel representation as in (2). A general result, yielding an algorithm for computing the state parameterizing the manifest behavior of a dynamical system from [12], is specialized here to a controller $\mathcal{C}$ by the following theorem.

Theorem 2: Given the manifest variable $s \in \mathbb{S}^T$, the following statements are equivalent:

1) The manifest variable s belongs to the controller behavior $\mathcal{C}$, i.e. $C(\frac{d}{dt})s = 0$
2) There exist an integer $\mathtt{n}_C$, a polynomial matrix $\chi \in \mathbb{R}^{\mathtt{n_c} \times \mathtt{s}}[\xi]$ and a state ζ such that $\zeta = \chi(\frac{d}{dt})s$

Proof: See [12, Theorem 6.2]. ∎

Note that the polynomial matrix χ in theorem 2 can be obtained by reduction of the kernel representation $C(\frac{d}{dt})s = 0$ to a first-order representation. An efficient algorithm is proposed in [12, Algorithm 1-3] to compute the polynomial matrix χ using iteratively the *shift-and-cut* operation(see [12, Definition 5.1]).

IV. Bumpless switching of a two-zone VRF system

A. Two-zone VRF benchmark description

The "physical" structure of a two-zone VRF system is depicted in figure 2.

The two-zone VRF system is a non-square multiple-input/multiple output system where the components of control vector $u = \begin{bmatrix} u_1 & u_2 & u_3 \end{bmatrix}^T$ are the two EEV openings $EEV_1 = u_1$ and $EEV_2 = u_2$ and the compressor speed $\omega_c = u_3$. The system outputs are the two superheat temperatures $T_s = \mathtt{col}(T_{s1}, T_{s1})$ (i.e., temperatures measured at points s_1 and s_2 respectively), the two evaporator temperatures $T_e = \mathtt{col}(T_{e1}, T_{e1})$ (i.e., temperatures measured at the entry e_1 and e_2 of each evaporator), and two zone temperatures $T_z = \mathtt{col}(T_{z1}, T_{z1})$. The controller structure of the two-zone system is basically similar to that proposed in [8] and illustrated in figure 3, where blue line corresponds to the reference trajectories and green line denotes the output trajectories of the plant. The feedback gain matrix K_e regulates the evaporator temperature T_e to its reference trajectory by using the compressor speed. Controllers K_s and K_z works under a master-slave arrangement which regulates T_z according to the user's setting, i.e. the reference trajectory $T_{z,ref}$. The master feedback loop with K_z produces a reference superheat temperature trajectory $T_{s,ref}$ to the slave feedback loop where K_s regulates T_s to its reference trajectory.

The prime aim of this control strategy is to regulate the cooling of two zones according to the user's setting in which the expansion valves play a key role, since they control the flow of refrigerant into the evaporator. The other two temperatures T_e and T_s are not strictly required to track the reference values from the perspective of cooling control. However, it is only sufficient to ensure that they stay within a reasonable band. In order to achieve these objectives, the controllers K_e, K_s, K_z can be synthesized either indirectly using the method presented in [8] or directly (i.e. as a pure data-driven controller) using the method presented in [5]. It is worth recalling that in this paper, the interest lies in demonstrating the effectiveness of the proposed bumpless switching algorithm instead of synthesizing the controllers.

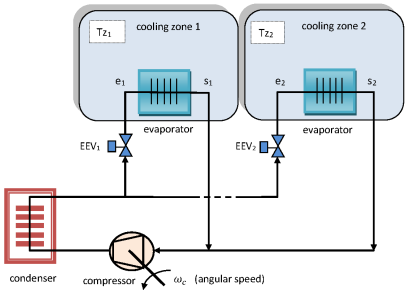

Fig. 2. Two-zone variable refrigerant flow system

B. *Simulations of the two-zone under mode-switching*

In order to demonstrate the effectiveness of the novel bumpless switching algorithm, we consider two modes of operation for the two-zone VRF system: Past mode in which only evaporator #1 is working, and future mode in which both evaporators are ON. For both of these modes, we are provided at the outset with a set of controllers given by

$$\mathcal{C}_{\mathtt{p}}: \begin{cases} K_e = \begin{bmatrix} 55.7 & 0 \end{bmatrix} \\ K_s = \xi^{-1} \times I_2 \times \begin{bmatrix} 0.0211(\xi + 0.043) & 0 \\ 0 & 0 \end{bmatrix} \\ K_z = \xi^{-1} \times I_2 \times \begin{bmatrix} 5(\xi + 0.0027) & 0 \\ 0 & 0 \end{bmatrix} \end{cases}, \mathcal{C}_{\mathtt{f}}: \begin{cases} K_e = \begin{bmatrix} 51.2676 & 54.5547 \end{bmatrix} \\ K_s = \xi^{-1} \times I_2 \begin{bmatrix} 0.018(\xi + 0.029) & 0 \\ 0 & 0.019(\xi + 0.02) \end{bmatrix} \\ K_z = \xi^{-1} \times I_2 \times \begin{bmatrix} 5(\xi + 0.0027) & 0 \\ 0 & 5(\xi + 0.0026) \end{bmatrix} \end{cases} \tag{6}$$

where I_2 is the identity matrix of order 2. During the control process, Evaporator #1 is always ON while Evaporator #2 is turned ON for 1800 sec (i.e. $t_{\mathtt{inter}} = 1800$sec) and turned OFF later. The temperature setting for zone #1 is always equal to 27 ^{0}C. During the ON state, the corresponding $T_{e,ref}$ is set to 10^0C and $T_{z2,ref}$ is set to 25^0C while during the OFF state, the corresponding $T_{e,ref}$ and $T_{z2,ref}$ are respectively set to 16^0C and 33^0C. The closed-loop responses are illustrated in figure 4. Observe that the temperature of zone 1 settles to the reference trajectory within 1000 sec while the temperature of zone 2 settles within 1800 sec. At time $t = 1800sec$, switching to another mode is demanded, so $T_{z2,ref}$ and $T_{e2,ref}$ are reset to their designated value. It is clear from the figures that in the direct switching, that is, when the state of the controller are not correctly initialized at the switching instant, we notice a significant bump which is an undesirable transient in the output of a two zone VRF system when it has already been settled.

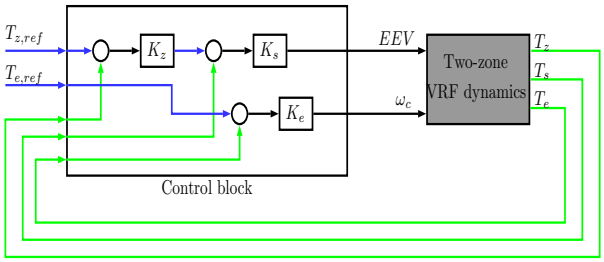

Fig. 3. Control strategy of the two-zone VRF system

V. Conclusions

A data-driven bumpless switching algorithm has been developed and implemented for managing the transients during mode switching control of a two-zone VRF air-conditioning system. It is shown that the direct switching between the different modes associated with the cooling demands gives rise to switching transients, which might negatively impact the indoor comfort and the energy efficiency of the overall system. With the proposed bumpless switching algorithm, no transients occur in the temperature of two zones. The novelty of this algorithm lies in its pure "data-driven" formulation that uses only the plant input/output measurements available in real-time. Looking at the effectiveness of the demonstrated mechanism, it is worth investigating in future the transient management under a series of mode switching control of a multi-zone VRF system.

Acknowledgment

The author would like to thank Professor Joseph Yamé for valuable discussion and collaboration on bumpless switching control.

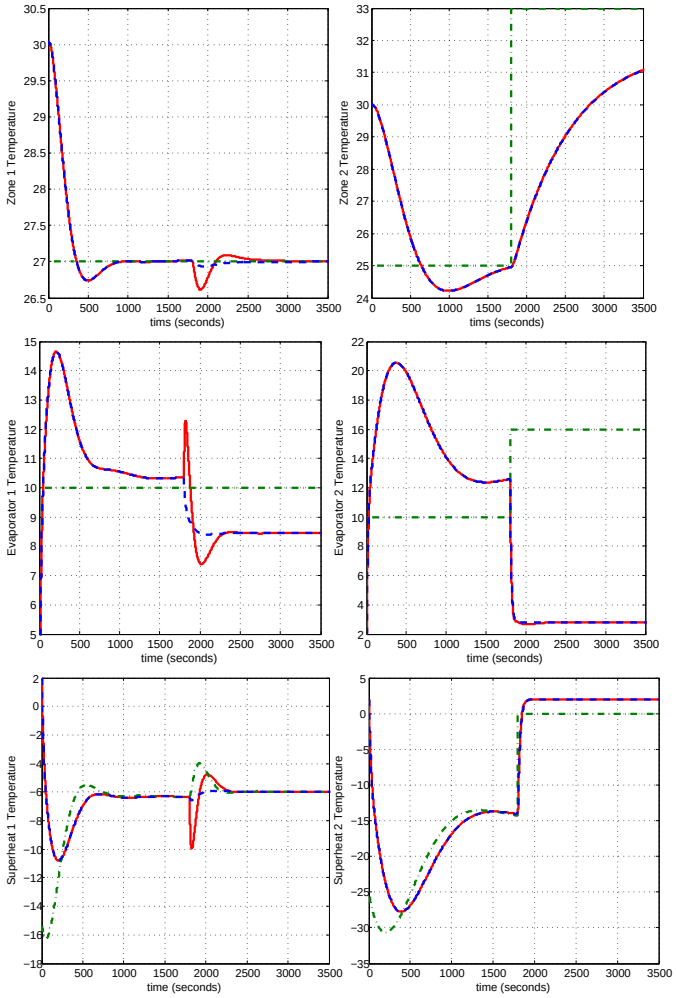

Fig. 4. Closed-loop responses: dash-dotted (green) line denotes the reference trajectory; solid (red) line denotes the bumpy output trajectories; dashed (blue) denotes the bumpless output trajectories

REFERENCES

[1] T. N. Aynur. Variable refrigerant flow systems: A review. *Energy and Buildings*, 42(7):1106–1112, July 2010.

[2] R. Bellman and K.L. Cooke. *Modern Elementary Differential Equations, Second Edition*. Dover Publications, Inc, 1995.

[3] W. Goetzler. Variable refrigerant flow systems. *ASHRAE Journal*, 49(4):24–31, 2007.

[4] S. F. Graebe and A. Ahlén. Bumpless transfer. In *The Control Handbook*, pages 381–388. IEEE Press, 1996.

[5] T. Jain, J. J. Yamé, and D Sauter. Trajectory-based real-time control of an electrical circuit against unknown faults. *Journal of the Franklin Institute, Elsevier*, 351(2):986–1000, 2014.

[6] Mitchell J.W. and Braun J.E. *Principles of Heating, Ventilation, and Air Conditioning in Buildings*. John Wiley & Sons, 2013.

[7] Zaccarian L. and Teel A.R. The $\mathcal{L}_2(\ell_2)$ bumpless transfer problem for linear plants: Its definition and solution. *Automatica*, 41:1273–1280, 2005.

[8] J.-L. Lin and T.-J. Yeh. Control of multi-evaporator air-conditioning systems for flow distribution. *Energy Conversion and Management*, 50:1529–1541, 2009.

[9] J.-L. Lin and T.-J. Yeh. Mode switching control of dual-evaporator air-conditioning systems. *Energy Conversion and Management*, 50:1542–1555, 2009.

[10] J. W. Polderman and J. C. Willems. *Introduction to Mathematical Systems Theory: A Behavioral Approach*. Springer-Verlag, 1997.

[11] Hanus R., Kinnaert M., and Henrotte J.L. Conditioning technique, a general anti-windup and bumpless transfer method. *Automatica*, 23:729–739, 1987.

[12] P. Rapisarda and J.C. Willems. State maps for linear systems. *SIAM Journal on Control and Optimization*, 35(3):1053–1091, 1997.

[13] P. Rocha and J. Wood. Trajectory control and interconnection of 1D and nD systems. *SIAM Journal on Control and Optimization*, 40(1):107–134, 2001.

[14] J. J. Yamé and M. Kinnaert. On bumps and reduction of switching transients in multicontroller systems. *Mathematical Problems in Engineering*, 2007:17, 2007.